frontiers | Frontiers in Marine Science

TYPE Original Research
PUBLISHED 29 November 2022
DOI 10.3389/fmars.2022.1056587

OPEN ACCESS

EDITED BY
Jun Gong,
Sun Yat-sen University, China

REVIEWED BY
Xiangrui Chen,
Ningbo University, China
Atef Omar,
Gangneung–Wonju National University, South Korea
Fengchao Li,
Hebei University, China

*CORRESPONDENCE
Jiamei Jiang
jm-jiang@shou.edu.cn

SPECIALTY SECTION
This article was submitted to Marine Evolutionary Biology, Biogeography and Species Diversity, a section of the journal Frontiers in Marine Science

RECEIVED 29 September 2022
ACCEPTED 31 October 2022
PUBLISHED 29 November 2022

CITATION
Zhang Z, Hines HN, Pan H and Jiang J (2022) The description of a new brackish water ciliate species from China, *Trachelostyla aestuarina* n. sp., with a species key and biogeographic investigation for *Trachelostyla* (Ciliophora, Sporadotrichida). *Front. Mar. Sci.* 9:1056587. doi: 10.3389/fmars.2022.1056587

The description of a new brackish water ciliate species from China, *Trachelostyla aestuarina* n. sp., with a species key and biogeographic investigation for *Trachelostyla* (Ciliophora, Sporadotrichida)

Zihui Zhang[1,2], Hunter N. Hines[3], Hongbo Pan[1,2] and Jiamei Jiang[1,2]*

[1]Shanghai Universities Key Laboratory of Marine Animal Taxonomy and Evolution, Shanghai Ocean University, Shanghai, China, [2]Engineering Research Center of Environmental DNA and Ecological Water Health Assessment, Shanghai Ocean University, Shanghai, China, [3]Harbor Branch Oceanographic Institute, Florida Atlantic University, Fort Pierce, FL, United States

The ciliated protists are a diverse group of microbial eukaryotes that play an important role in the functioning of microbial food webs. The genus *Trachelostyla* Borror, 1972, comprised a few species with a non-twisted distinctly cephalized shape. The overall taxonomy has been challenging for this group, and the understanding of their diversity and distribution is therefore relatively limited. To further investigate this group, we report here on two species from the East China Sea, *Trachelostyla aestuarina* n. sp. and *Trachelostyla caudata* Borror, 1972, including their *in vivo* morphology, infraciliature, and phylogenetic relationships based on 18S rRNA gene sequences. The physiological reorganization stages of the latter were also investigated. *T. aestuarina* is characterized by a combination of features including a bipartite cell shape, a size of 150–220 × 15–35 μm, scattered cortical granules, and multiple macronuclear nodules (37–55). *T. caudata* has only 10 cirri in the frontal region, fewer than its congeners; thus, we improved the definition of the genus. The global distribution of *Trachelostyla* was summarized based on the available literature and a key to the valid species provided. This work improves the overall knowledge of hypotrich biodiversity and provides underpinning for future researchers in global regions for environmental monitoring and resource investigations.

KEYWORDS

ciliated protists, distribution, morphogenesis, phylogeny, taxonomy

1 Introduction

The ciliated protists are an interesting and diverse group of single-cell microbial eukaryotes that play an important role in microbial food webs and are also useful as model organisms in studies of development, evolution, and molecular biology (Obert and Vďačný, 2020; Park et al., 2020; Song et al., 2021; Vďačný and Foissner, 2021; Ahsan et al., 2022; Timmons et al., 2022; Valentine and Van Houten, 2022; Zhang et al., 2022b). Hypotrichs (subclass Hypotricha Stein, 1859) are a complex group of ciliates that are frequently studied but, despite this (or perhaps because of this), remains one of the most confusing groups with respect to their taxonomic and phylogenetic relationships (Chen et al., 2020; Kim et al., 2020; Li et al., 2021; Luo et al., 2021; Omar et al., 2022; Wu et al., 2022; Xu et al., 2022).

Trachelostyla Borror, 1972, is a small group of hypotrichs with 18 frontal–ventral–transverse (FVT) cirri and a non-twisted cell that is distinctly cephalized. It was established with two species, namely, *Trachelostyla* (*Stichochaeta*) *pediculiformis* (Cohn, 1866) Kahl, 1932, and *Trachelostyla caudata* Kahl, 1932. However, Kahl did not designate the type species; thus, the genus was invalid until Borror (1972) fixed *T. pediculiformis* as the type species (Berger, 1999). Compared with other hypotrichous ciliates, species of the genus *Trachelostyla* are less frequently reported, and their identification is challenging owing to their similar general morphology, especially when the protargol-impregnated specimens and molecular data are unavailable (Berger, 2008; Zhang et al., 2022a).

Here, we describe a new species of *Trachelostyla*, *Trachelostyla aestuarina* n. sp., and reinvestigate *T. caudata* based on a Chinese population, completing its ciliary analysis and physiological reorganization features. We also present their phylogenetic relationships inferred from small subunit ribosomal RNA (SSU rRNA) gene sequence data. Furthermore, a key to the identification of the five valid species is provided and the global biogeography of the genus *Trachelostyla* summarized based on previous reports and the data presented here.

2 Materials and methods

2.1 Sampling and cultivation

T. aestuarina n. sp. was collected on July 15, 2021, from the mudflat of the Yangtze River Estuary, Nanhuizui Guanhai Park, Shanghai, China (30°54′47.3" N, 121°58′45.6" E). A Xylem ProQuatro YSI was used to obtain water metadata; the water temperature was 33.7°C, the salinity was 8.63‰, and the pH was 8.44 at the time of sampling. Pore water and substrate were collected by digging a pit about 10 cm deep. The mud samples were maintained at room temperature (20–24°C) in glass Petri dishes using habitat water with rice grains to enrich the growth of bacterial food for the ciliates. *T. aestuarina* n. sp. appeared after 1 week in the sediment in one Petri dish, when the salinity increased to 11‰ due to evaporation.

T. caudata (Kahl, 1932) Borror, 1972, was collected on March 13, 2021, from the top 5 cm of sandy sediments at a water depth of 14–15 m of the East Sea, China (30°54′58.4" N, 122°29′36.1" E). The sample was collected onboard of R/V "Zheyuke 2" during the open research cruise NORC2021-03 using a Van Veen grab. The water temperature (10.9°C), salinity (29.39‰), and the pH (7.78) were recorded using a CTD (conductivity, temperature, depth) at the time of sampling. Using artificial seawater (30‰) for cultivation, the culture conditions were the same as above. *T. caudata* appeared after about 2 weeks.

2.2 Morphology and physiological reorganization

Living cells were observed using an Olympus BX53 microscope and Olympus DP73 camera with the cellSens program. Bright-field and differential interference contrast microscopy at magnifications from ×40 to ×1,000 were used for the investigations. The protargol method (Wilbert, 1975) was used to reveal the ciliary pattern and the nuclear apparatus with the protargol reagent manually synthesized according to Pan et al. (2013). The counts and measurements of impregnated specimens were performed at ×1,000 magnification. Drawings were made with the aid of a camera lucida and the computer program Photoshop. To illustrate the changes occurring during the physiological reorganization process, parental cirri were depicted with contour lines, whereas new ones were shaded black. General terminology was according to Lynn (2008), while classification followed Berger (2008) and Paiva (2020).

2.3 Geographical distribution analyses

Information on the global distribution patterns of the species within *Trachelostyla* was derived from previous studies, which included morphological descriptions and recognizable illustrations, as well as records not substantiated by morphological data. The literature used during analysis was mainly from Berger (2008).

2.4 DNA extraction and gene sequencing

In order to remove potential contamination, the cells were washed five times with filtered (0.22 μm) habitat water using a

micropipette, and then a single cell of each species was transferred to a 1.5-ml centrifuge tube with a minimum amount of water. Genomic DNA was extracted using the DNeasy Blood and Tissue Kit (Qiagen, Hilden, Germany) using one-fourth volume of the manufacturer's instructions. The SSU rRNA gene sequences were amplified using the universal eukaryotic primers Euk A (forward: 5′-AACCTGGTTGATCCTGCCAGT-3′) and Euk B (reverse: 5′-TGATCCTTCTGCAGGTTCACCTAC-3′) (Medlin et al., 1988). Using the C2000 Touch™ Thermal Cycler from Bio-Rad (Hercules, CA, USA), the PCR conditions for the amplification of the SSU rRNA gene sequences were as follows: 30 s initial denaturation (98°C), followed by 34 cycles of 10 s at 98°C, 30 s at 69°C, and 1 min at 72°C, with a final extension of 5 min at 72°C (Chen et al., 2022). The PCR products were sent for commercial cloning and sequencing (Sangon, Shanghai, China) using primers M13F and M13R and one internal primer, Pro+930 (5′-GGTTAAAAAGCTCGTAGT-3′). Contigs were assembled using Seqman v.7.1.0 (44.1) (DNASTAR Madison, WI, USA).

2.5 Phylogenetic analyses

The SSU rRNA gene sequences of *T. aestuarina* n. sp. and *T. caudata* (Kahl, 1932) Borror, 1972, were blasted against the nucleotide National Center for Biotechnology Information (NCBI) database. The two new sequences were aligned together with 79 other spirotrich sequences, including four euplotids as outgroup taxa, downloaded from the NCBI database.

The sequences were aligned using the MUSCLE algorithm in MEGA v11.0.8 (Tamura et al., 2021) with the default parameters. Gblocks 0.91b (Castresana, 2000) was used for alignment masking. The final alignment (1,686 bp long) was used to construct the phylogenetic trees. Maximum likelihood (ML) analysis was carried out using RAxML-HPC2 on XSEDE v8.2.12 (Stamatakis, 2014) on the CIPRES Science Gateway web server (Miller et al., 2011) employing the GTRGAMMA model with 1,000 bootstrap replicates. Bayesian inference (BI) analysis was performed with MrBayes on XSEDE v3.2.7a (Ronquist et al., 2012). The best-fit model, TIM2+I+G, was selected as the best model with the Akaike information criterion (AIC) in JModeltest2 on XSEDE v2.2.6 for BI analysis. Markov chain Monte Carlo simulations were run for 1,000,000 generations with a sampling frequency of 100, and the first 25% (2,500) of each run were discarded as burn-in. The remaining trees were used to calculate the posterior probabilities with a majority-rule consensus. Trees were visualized using FigTree 1.4.3 (Rambaut, 2018).

2.6 ZooBank registration numbers

Present work: urn:lsid:zoobank.org:pub:E10BA883-FAC7-4E81-8CB4-D521A945D99F

Trachelostyla aestuarina n. sp.: urn:lsid:zoobank.org:act:C8801538-91D8-430A-94F0-FD6E58B9F4E3

3 Results

Subclass Hypotricha Stein, 1859
Order Sporadotrichida Fauré-Fremiet, 1961
Family Trachelostylidae Small and Lynn, 1985
Genus *Trachelostyla* Borror, 1972

3.1 Diagnosis of the genus is improved based on the infraciliature of *T. caudata* (present study)

The cell is dorsoventrally flattened, nonspirally twisted, and is elongate with a conspicuously narrowed peristomal region. The ciliature is generally in a 10:2:5:3 or 11:2:5:3 pattern, i.e., with 10 or 11 cirri in the frontal region (three frontal cirri, four front oventral cirri, one buccal cirrus, and two or three postoral ventral cirri), two pretransverse ventral cirri located anterior to five transverse cirri, and three well-differentiated caudal cirri. One left and one right row of marginal cirri are not confluent posteriorly.

3.2 *Trachelostyla aestuarina* n. sp.

3.2.1 Diagnosis

The cell is flexible, elongated, and bipartite, 150–220 × 15–35 μm *in vivo*. The cortical granules are spherical, colorless, and arranged in short lines along dorsal kineties, with one non-contractile vacuole. There are 42–59 adoral membranelles, three frontal cirri, one buccal cirrus, four frontoventral cirri, three postoral ventral cirri, two pretransverse cirri, five transverse cirri, 25–40 left and 30–47 right marginal cirri, three caudal cirri, six dorsal kineties, 37–55 macronuclear nodules, and one to five micronuclei. The cell was found within a brackish water habitat.

3.2.2 Type locality

Mudflat of the Yangtze River Estuary, Nanhuizui Guanhai Park, Shanghai, China (30°54′47.3"N, 121°58′45.6" E).

3.2.3 Type specimen

A protargol slide containing the holotype specimen (registration no. ZZH20210715-1) (see Figures 1F, G, 2N) and

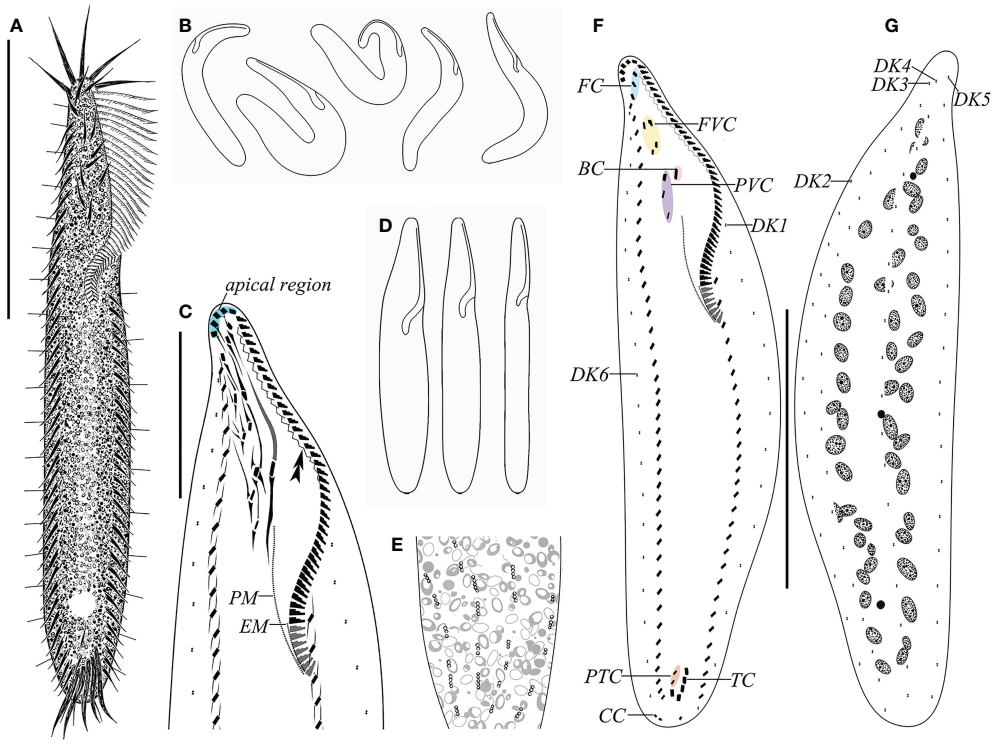

FIGURE 1
Morphology and ciliature of *Trachelostyla aestuarina* n. sp. from life **(A, B, E)** and after protargol impregnation **(C, F, G)**. **(A)** Ventral view of an ideal representative individual. **(B)** Different outlines showing the flexibility of the cell. **(C)** Detailed infraciliature of the anterior region. *Double arrowhead* shows the zigzag fiber. **(D)** Different cell shapes. **(E)** Partial dorsal view showing the distribution of the cortical granules. **(F, G)** Ventral **(F)** and dorsal **(G)** views of the holotype specimen showing the ciliary pattern and the nuclear apparatus. *BC*, buccal cirrus; *CC*, caudal cirri; *EM*, endoral membrane; *FC*, frontal cirri; *FVC*, frontoventral cirri; *PM*, paroral membrane; *PTC*, pretransverse ventral cirri; *PVC*, postoral ventral cirri; *TC*, transverse cirri; *DK1–DK6*, dorsal kineties 1–6. *Scale bars*, 80 μm **(A, F, G)** and 30 μm **(C)**.

one paratype slide (registration no. ZZH20210715-2) have been deposited in the Laboratory of Protozoology, Shanghai Ocean University, China.

3.2.4 Etymology

The species-group name "*aestuarina*" refers to the habitat (Yangtze River Estuary) where the species was collected.

3.2.5 Morphological description of *Trachelostyla aestuarina* n. sp.

The cell size *in vivo* is 150–220 × 15–35 μm, bipartite, and the trunk shows an elongate ellipsoidal shape, with a round posterior end but with a narrow neck-like constriction at the anterior one-fifth to one-fourth of the cell length. At low magnification, the cell appears dark gray and opaque, flexible but not contractile (Figures 1A–C, 2A–F). The cytoplasm is colorless, usually packed with numerous irregularly shaped granules, about 3 μm across. The mid-ventral region forms a longitudinal concavity from the end of the adoral zone terminating at the posterior one-sixth of the cell (Figure 2H). Since this depression contains less cytoplasm, it is more transparent than other parts of the cell. The vacuole is about 8 μm in diameter at the end of depression, but with no contraction observed (Figures 2B, C, H). The cortical granules are of a single type, spherical (about 0.5 μm in size), colorless, with three to six linearly arranged in six lines along the dorsal kineties (Figures 1E, 2L). As many as 37–55 macronuclear nodules, ovoid or ellipsoidal, 2–4 μm long after protargol impregnation, are scattered throughout the cytoplasm (Figures 1G, 2M, N and Table 1). There are one to five micronuclei (Figures 1G, 2N). The ciliate crawls rapidly on debris particles, often making lively short movements, and occasionally stopping.

The adoral zone occupies 30%–44% of the cell length *in vivo* and 40%–52% in protargol preparations, contains 42–59 membranelles, and is composed of apical and lapel regions (Figures 1A, F, 2A–D, G, I, N). The apical region includes five 15- to 26-μm-long strong and radially extending membranelles. Lapel membranelles are densely arranged along the left edge of the anterior end of the cell, relatively thin. The fibril is zigzag-shaped, arranged along the adoral zone (Figures 1C, F, 2P).

10.3389/fmars.2022.1056587

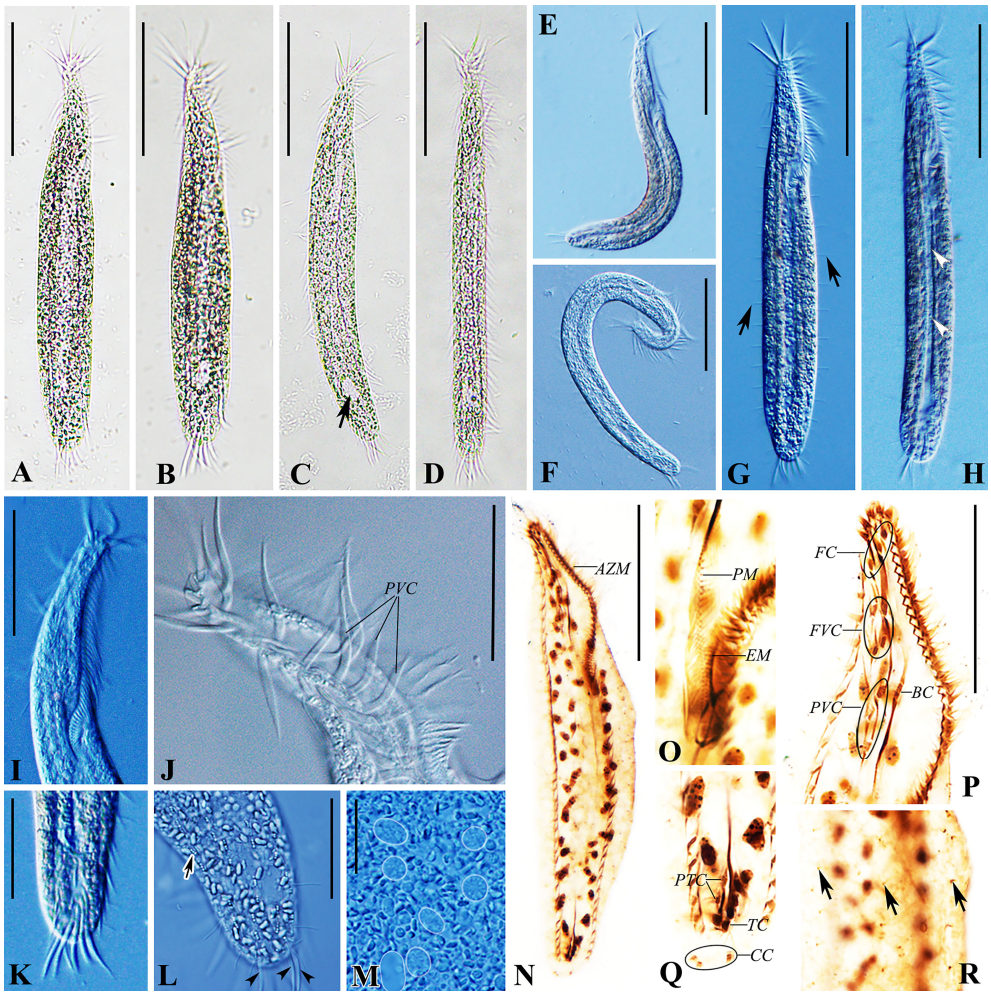

FIGURE 2
Trachelostyla aestuarina n. sp. from life [bright field **(A–D)** and differential interference contrast **(E–M)**] and after protargol impregnation **(N–R)**. **(A–H)** Ventral views of individuals showing different cell shapes and degree of flexibility. *Arrow* in **(C)** marks the non-contractile vacuole, *arrows* in **(G)** mark the rows of dorsal bristles, and *arrowheads* in **(H)** show the longitudinal concavity of the cell. **(I)** Anterior section showing the shape of the adoral zone of membranelles. **(J)** Arrangement of cirri near the oral region. **(K)** Ventral view of the posterior section showing transverse cirri. **(L)** Dorsal view of the posterior section. *Arrows* indicate cortical granules, while *arrowheads* mark the caudal cirri. **(M)** Macronuclear nodules (white outlines added to 7 Ma). **(N)** Ventral view of the holotype showing the ciliary pattern and the nuclear apparatus. **(O)** Ventral view of the buccal region marking the undulating membranes. **(P)** Ventral view of the oral region. **(Q)** Ventral view of the posterior cell region. **(R)** Partial dorsal view. *Arrows* indicate dorsal bristles. *AZM*, adoral zone of membranelles; *BC*, buccal cirrus; *CC*, caudal cirri; *EM*, endoral membrane; *FC*, frontal cirri; *FVC*, frontoventral cirri; *PM*, paroral membrane; *PTC*, pretransverse ventral cirri; *PVC*, postoral ventral cirri; *TC*, transverse cirri. *Scale bars*, 60 μm **(A–N)**, 30 μm **(I, J, P)**, 25 μm **(K, L)**, and 8 μm **(M)**.

Undulating membranes are not obvious, arranged almost in parallel. The paroral starts at the level of the last postoral ventral cirrus and terminates at the buccal vertex; the endoral extends from the mid-portion of the paroral to the end of the adoral membranelles (Figures 1D, F, 2O).

FVT cirri are in a constant 3:1:4:3:2:5 pattern (three frontal, one buccal, four frontoventral, three postoral ventral, two pretransverse ventral, and five transverse). Consistently, there are 11 cirri in the frontal area, densely arranged in the anterior two-thirds of the adoral zone, about 20 μm long *in vivo*, and associated with fiber bundles. Three frontal cirri are arranged behind the apical adoral and near the distal end of the adoral zone. One buccal cirrus is situated at the level of the mid-portion of the adoral zone and directly above the paroral. Four frontoventral cirri are located posterior to the rightmost frontal cirrus and anterior to the level of the fifth right marginal cirrus, forming a roughly rectangular pattern. Three postoral ventral cirri are aligned longitudinally, the first located right to the buccal cirrus and the last placed in the right side of the apex of the paroral (Figures 1C, F, 2J, P). Two pretransverse

10.3389/fmars.2022.1056587

TABLE 1 Morphometric characteristics of *Trachelostyla aestuarina* n. sp. (upper line) and the Chinese population of *Trachelostyla caudata* (lower line).

Character	Min	Max	Mean	*M*	SD	CV (%)	*n*
Cell length (μm)	122	190	147.5	144.5	18.29	12.4	20
	73	126	103.5	101.5	13.21	12.8	20
Cell width (μm)	25	42	35.7	36.0	4.04	11.3	20
	21	37	28.3	28.5	4.42	15.7	20
Adoral zone of membranelles, length (μm)	56	72	64.4	65.0	4.46	6.9	20
	39	50	46.3	47.0	3.28	7.1	20
Adoral membranelles, number	42	59	49.9	49.5	4.30	8.6	20
	30	45	37.5	37.0	3.83	10.2	20
Frontal cirri, number	3	3	3.0	3.0	0.00	0.0	20
	3	3	3.0	3.0	0.00	0.0	20
Frontoventral cirri, number	4	4	4.0	4.0	0.00	0.0	20
	4	4	4.0	4.0	0.00	0.0	20
Buccal cirrus, number	1	1	1.0	1.0	0.00	0.0	20
	1	1	1.0	1.0	0.00	0.0	20
Postoral ventral cirri, number	3	3	3.0	3.0	0.00	0.0	20
	2	2	2.0	2.0	0.00	0.0	20
Pretransverse ventral cirri, number	2	2	2.0	2.0	0.00	0.0	20
	2	2	2.0	2.0	0.00	0.0	20
Transverse cirri, number	5	5	5.0	5.0	0.00	0.0	20
	5	5	5.0	5.0	0.00	0.0	20
Left marginal cirri, number	25	40	30.6	28.5	4.63	15.1	20
	14	30	22.5	22.0	4.33	19.3	20
Right marginal cirri, number	30	47	38.2	37.5	4.28	11.2	20
	18	40	30.7	30.0	5.67	18.5	20
Caudal cirri, number	3	3	3.0	3.0	0.00	0.0	20
	3	3	3.0	3.0	0.00	0.0	20
Dorsal kineties, number	6	6	6.0	6.0	0.00	0.0	20
	6	6	6.0	6.0	0.00	0.0	20
Macronuclear nodules, number	37	55	49.2	50.5	4.93	10.0	20
	20	33	24.8	24.0	3.91	15.8	20
Macronuclei, largest diameter (μm)	2	4	2.8	3.0	0.83	29.8	20
	2	6	3.3	3.0	1.02	31.4	20
Micronuclei, number	1	6	2.5	2.0	1.61	64.2	20
	1	5	2.5	2.0	1.15	46.8	20

Mean, arithmetic mean; M, median; SD, standard deviation; CV, coefficient of variation; Min, minimum; Max, maximum; n, number of individuals examined.

ventral cirri are vertically aligned, located above the rightmost transverse cirrus. Five transverse cirri are arranged in a "J"-shaped pattern, projecting beyond the posterior cell margin, about 24 μm long *in vivo* (Figures 1F, 2K, Q).

There is one left and one right marginal cirral row comprised 25–40 and 30–47 cirri, respectively. The left marginal cirral row begins slightly above the buccal vertex and terminates at the level of the posteriormost transverse cirrus. The right marginal row extends from below the rightmost frontal cirrus to the same level of the left marginal row end (Figures 1F, 2N and Table 1).

Dorsal kineties (DKs) are composed of six rows of stiff and conspicuous bristles, 7–8 μm in length. DK1 and DK2 start at about one-fourth and one-fifth of the cell anterior end, respectively, and terminate at the end of the cell. The others (DK2 and DK4–DK6) extend over the whole length of the cell (Figures 1F, G, 2G). Three inconspicuous caudal cirri, 13–17 μm in length, are in the leftmost cirrus apart from the other two (Figures 1F, 2L).

3.3 *Trachelostyla caudata* (Kahl, 1932) Borror, 1972

3.3.1 Morphological description

The cell size is 55–125 × 10–25 μm *in vivo*, usually about 100 × 18 μm. The cell shape is elongate and tripartite, with a narrow neck-like constriction at the anterior one-fourth of the

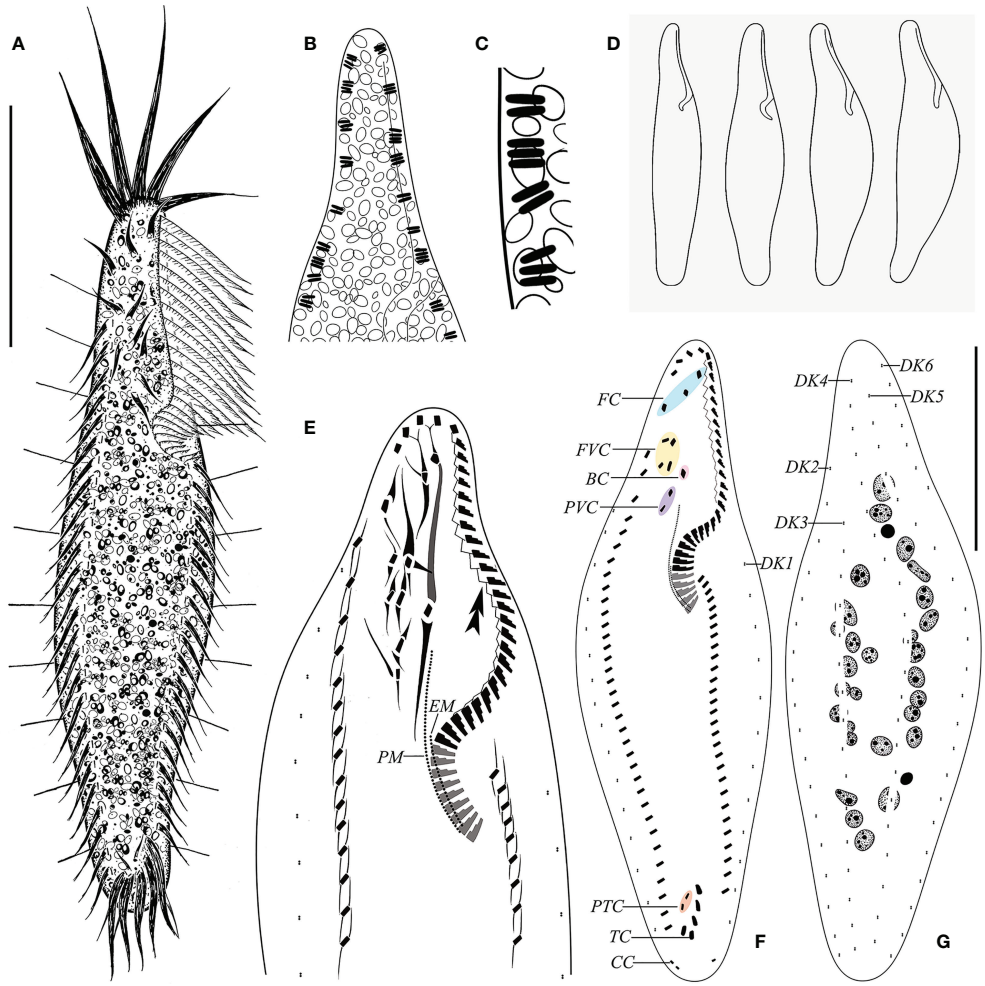

FIGURE 3
Morphology of *Trachelostyla caudata* from life **(A–D)** and after protargol impregnation **(E–G)**. **(A)** Ventral view of an ideal representative individual. **(B)** Arrangement of extrusomes (*dark shading*). **(C)** Rod-like extrusomes. **(D)** Different cell shapes. **(E)** Detailed infraciliature of the anterior region. *Double arrowhead* shows zigzag fiber. **(F, G)** Ventral **(F)** and dorsal **(G)** views showing the ciliary pattern and the nuclear apparatus. *BC*, buccal cirrus; *CC*, caudal cirri; *EM*, endoral membrane; *FC*, frontal cirri; *FVC*, frontoventral cirri; *PM*, paroral membrane; *PTC*, pretransverse ventral cirri; *PVC*, postoral ventral cirri; *TC*, transverse cirri; *DK1–DK6*, dorsal kineties 1–6. *Scale bar*, 35 μm.

cell length, 5–9 μm wide, accounting for one-third to one-half of the cell width. The posterior one-fourth of the cell is slightly tail-like, narrowed, 7–13 μm wide, one-half to four-fifths of the cell width. The ventral surface is flat or slightly concave, the dorsal side usually arched at the middle of the cell, slightly bendable, but not retractable (Figures 3A, D, 4A–D). The cell is colorless to light gray, with numerous densely arranged, irregularly shaped, colorless endoplasmic particles, 1–2.5 μm in diameter. The extrusomes are rod-shaped, about 1.5 μm long, scattered along the cell margin in groups (Figures 3B, C, 4G). The cell lacks cortical granules, and no contractile vacuole was observed. The presence of cysts was not observed before the emergence of the species or after the decline of the population. Conjugation was not observed. Twenty to 33 ovoid or ellipsoidal macronuclear nodules, 2–6 μm long each after protargol impregnation, are arranged in a ring-like pattern, one to five micronuclei, scattered among macronuclei (Figures 3G, 4H, K). The cell feeds on bacteria and was usually observed resting on the bottom of the Petri dish substrate or moving slowly.

The adoral zone of membranelles (AZM) occupies about 30% of the cell length *in vivo* (Figures 3A, 4F) and 38%–52% in protargol preparations (Figures 3F, 4H). The AZM is composed of 30–45 membranelles, which form two groups of different forms: the apical region composed of five membranelles, 16–22 μm long, stout and radially extending, and the lapel's membranelles, which are conspicuously thinner, about 10 μm long (Figures 3A, E, F, 4A–D, F, H, I). The base of the largest membranelle is approximately 3 μm wide. A zigzag structure

10.3389/fmars.2022.1056587

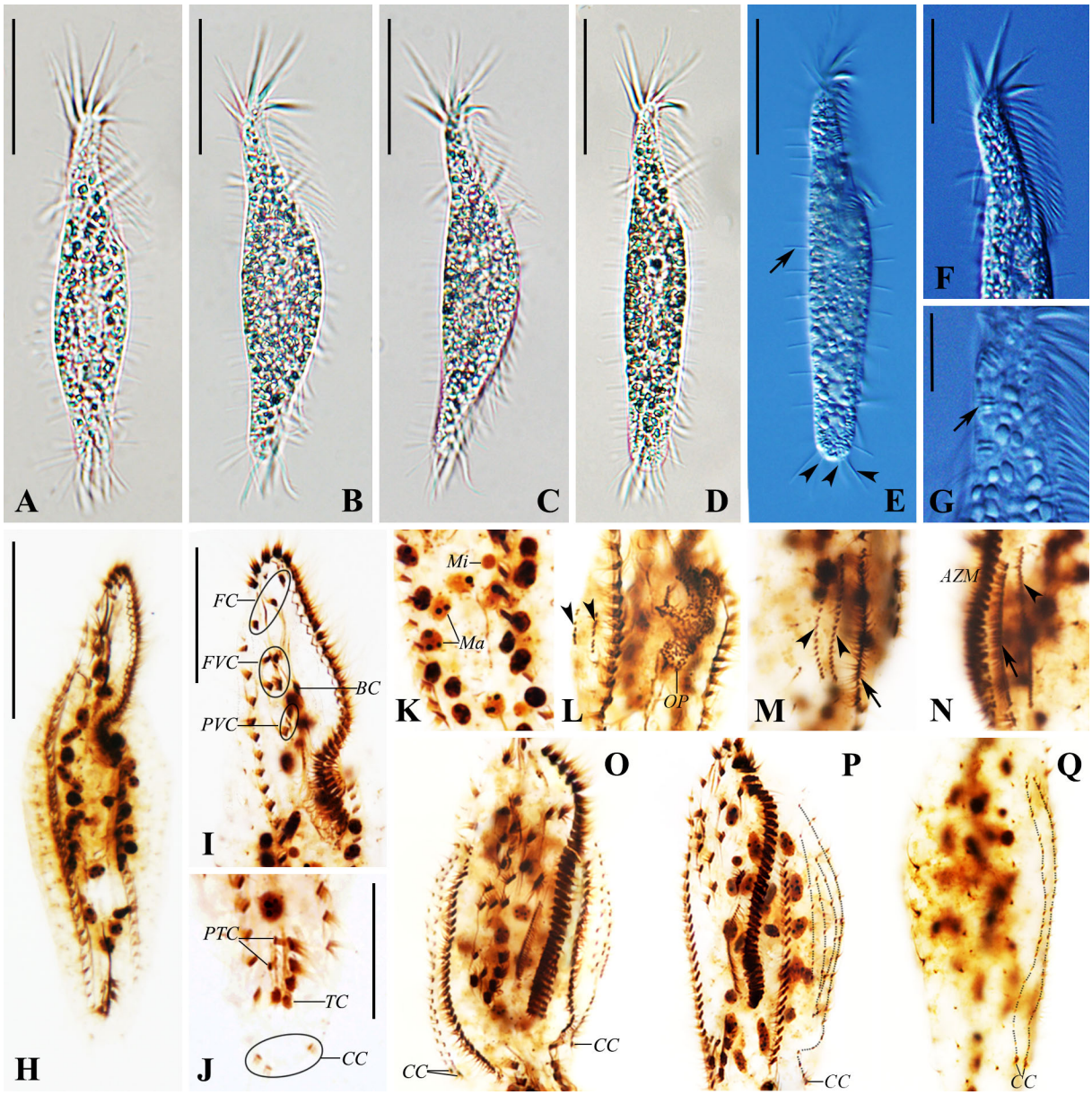

FIGURE 4
Photomicrographs of *Trachelostyla caudata* from life [bright field **(A–D)** and differential interference contrast **(E–G)**] and after protargol staining **(H–Q)**. **(A–E)** Ventral views of different individuals showing variations in cell shape. *Arrow* in **(E)** marks the row of dorsal bristles, while *arrowheads* in **(E)** indicate three caudal cirri. **(F)** Anterior section showing the shape of the adoral zone of membranelles. **(G)** Ventral view. *Arrow* shows extrusomes. **(H)** Ventral views of the paratype specimen showing the ciliary pattern and the nuclear apparatus. **(I)** Ventral view of the anterior region. **(J)** Ventral view of the posterior cell region. **(K)** Macronuclear nodules and micronuclei. **(L)** Ventral view of an early reorganizer showing the oral primordium and dorsal kinety anlagen (*arrowheads*). **(M, N)** Right **(M)** and left **(N)** lateral views of an early-to-mid reorganizer. *Arrows* indicate marginal anlagen, while *arrowheads* show dorsal kinety anlagen. **(O–Q)** Ventral **(O, P)** and dorsal **(Q)** views of late organizers. *AZM*, adoral zone of membranelles; *BC*, buccal cirrus; *CC*, caudal cirri; *FC*, frontal cirri; *FVC*, frontoventral cirri; *Ma*, macronuclear nodules; *Mi*, micronuclei; *OP*, oral primordium; *PTC*, pretransverse ventral cirri; *PVC*, postoral ventral cirri; *TC*, transverse cirri; *DK1–DK6*, dorsal kineties 1–6. *Scale bars*, 35 μm **(A–H)**, 20 μm **(F I, J)**, and 6 μm **(G)**.

composed of fibrils is always positioned along the right of lapel membranelles. Undulating membranes are arranged almost in parallel, the paroral extending from below the level of the anteriormost postoral ventral cirrus to the end of adoral membranelles, the endoral starting at mid-portion of the paroral, also ending at the buccal vertex (Figure 3E).

The FVT cirral pattern is invariably in 3:1:4:2:2:5 (three frontal, one buccal, four frontoventral, two postoral ventral, two pretransverse ventral, and five transverse). The frontal–ventral cirri are surrounded by many thick fibers (Figures 3E, 4I). Three frontal cirri are arranged behind apical adoral membranelles, away from the distal end of the adoral zone. One buccal cirrus is situated at the level of the mid-portion of the adoral zone and directly above the paroral. Four frontoventral cirri are located posterior to the rightmost frontal cirrus, forming a roughly rectangular pattern, and the two roots at the back are slightly anterior to the level of the buccal cirrus. Two postoral ventral cirri are aligned longitudinally and located right to the anterior portion of the paroral (Figures 3A, E, F, 4I). Two pretransverse ventral cirri are obviously weak. Five transverse cirri are arranged in a "J"-shaped pattern, projecting beyond the posterior cell margin, about 13–17 μm long *in vivo* (Figures 3F, 4A–D, J).

One right marginal row is composed of 18–40 cirri, beginning at the anterior one-fifth of the cell length, ending near the rightmost transverse cirrus. One left marginal row is composed of 14–30 cirri, starting slightly above the buccal vertex and terminating at the level of the leftmost transverse cirrus (Figures 3F, 4H and Table 1). Cirri are about 13 μm long *in vivo* (Figure 3A).

Dorsal bristles are very distinct, rigid, about 6 μm long *in vivo*, and arranged in six longitudinal kineties (Figures 3A, F, G and 4E). DK1 is relatively shorter, initiating at about one-third of the cell anterior end and terminating at the level of the middle transverse cirrus. DK2 and DK3 start at about one-fifth of the cell anterior end and terminate at the end of the cell. The remaining three kineties (DK4–DK6) extend over the whole length of the cell. There are three caudal cirri, about 9 μm long *in vivo*, each located at the end of DK4, DK5, and DK6 (Figures 3F, G).

3.3.2 Physiological reorganization

One early and one early-to-mid stage reorganizers, as well as three late-stage reorganizers, were found in protargol preparations of *T. caudata*.

The oral primordium formed *de novo* as a field of anarchic groups of basal bodies in the middle of the cell, which probably gave rise to the anlagen of undulating membranes. The anterior end originates at the level of the posterior fourth parental adoral membranelles. The oral primordium is produced in epiapokinetal, as it forms and develops on the cell surface (Figures 4L, 5A).

Parental structures gradually migrate to the upper right in the formation of FVT cirral anlagen (FVT-anlagen). FVT-anlagen I–VI generate 1:3:3:3:3:4 cirri, respectively. Three frontal cirri originate from the anterior end of FVT-anlagen I–III (I/1, II/3, and III/3). One buccal cirrus is formed from FVT-anlage II (II/2). Four frontoventral cirri develop from FVT-anlagen III, IV, and VI. FVT-anlagen III and IV each produce one frontoventral cirrus, while FVT-anlage VI forms two cirri

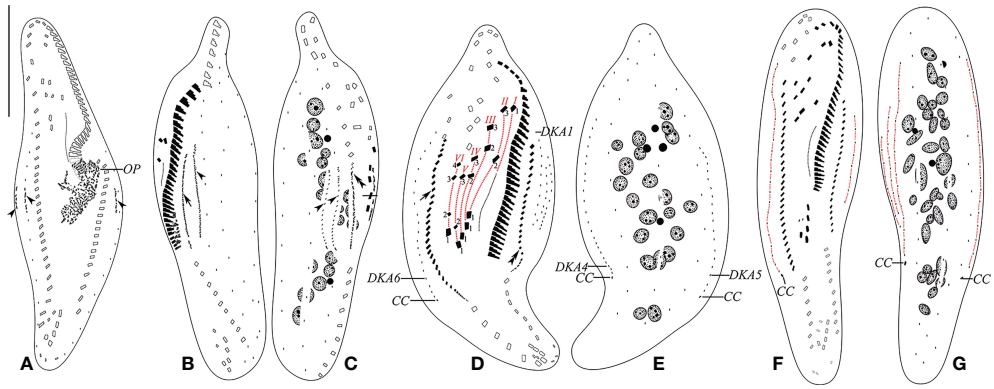

FIGURE 5
(A–G) Early **(A)**, early-to-mid **(B, C)**, late mid **(D, E)**, and late **(F, G)** stages of physiological reorganization after protargol impregnation. **(A)** Ventral view of an early reorganizer showing oral primordium and dorsal kinety anlagen (*arrowheads*). **(B, C)** Left **(B)** and right **(C)** lateral views of an early-to-mid reorganizer. *Arrow* indicates left marginal anlage, *double arrowhead* indicates right marginal anlage, and *arrowheads* show dorsal kinety anlagen. **(D, E)** Ventral **(D)** and dorsal **(E)** views of a slightly later reorganizer. *Arrow* indicates right marginal anlage, while *double arrowhead* shows left marginal anlage. Frontal–ventral–transverse cirri originating from the same anlagen are connected by a *red dotted line*. **(F, G)** Ventral **(F)** and dorsal **(G)** views of a late reorganizer. *CC*, caudal cirri; *DKA1, 4–6*, first, fourth, fifth, and sixth dorsal kinety anlage; *OP*, oral primordium; *I–VI*, frontal–ventral–transverse cirri originating from anlagen I–VI. *Scale bar*, 35 μm.

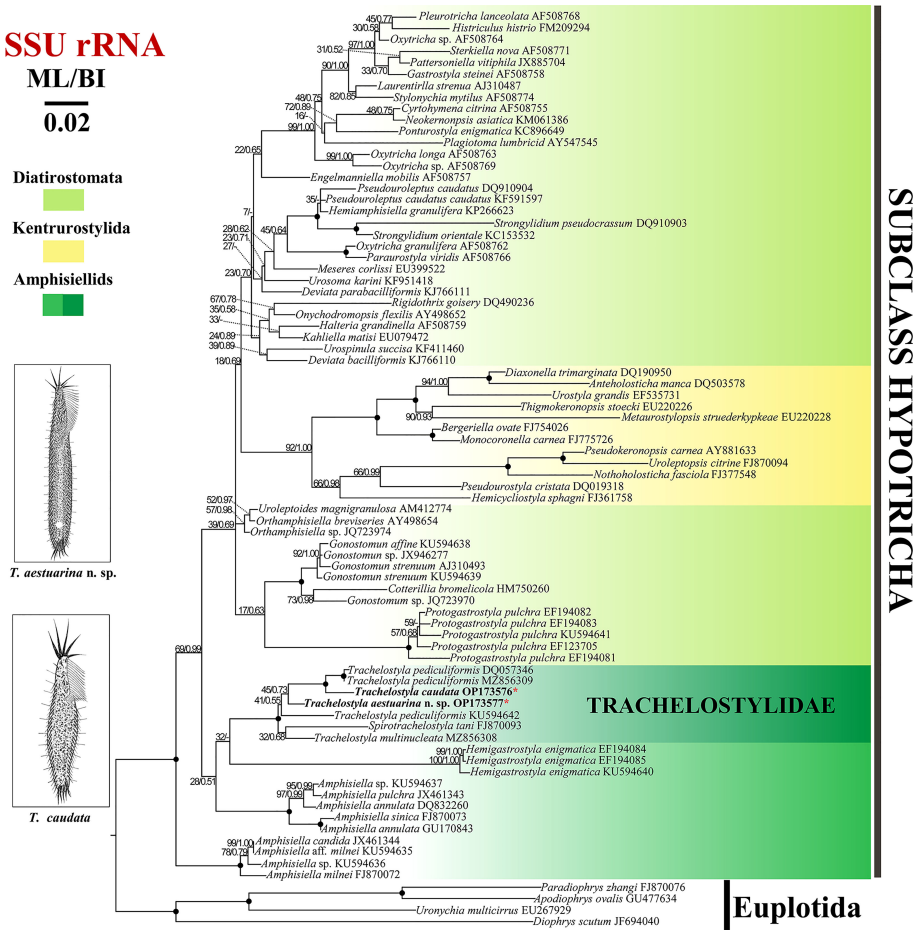

FIGURE 6
Maximum likelihood (ML) tree inferred from small subunit (SSU) rRNA gene sequences showing the phylogenetic positions of *Trachelostyla aestuarina* n. sp. and *Trachelostyla caudata* Chinese population (*asterisk in red*). *Numbers near branches* denote bootstrap values for ML and posterior probabilities for Bayesian inference (BI). *Dash* indicates the disagreement between the ML and BI trees. Fully supported (ML/BI, 100/1.00) branches are marked with *solid circles*. The GenBank accession numbers are provided *after species names*. *Scale bar* corresponds to three substitutions per 100 nucleotide positions.

(III/2, IV/3, VI/4, and VI/3, respectively). Two postoral ventral cirri are derived from FVT-anlagen IV and V (IV/2 and V/3). Two pretransverse ventral cirri are generated from FVT-anlagen V and VI (V/2 and VI/2). FVT-anlagen II–VI each form a transverse cirrus posteriorly (II–VI/1) (Figures 4O, P, 5D, F). The new undulating membranes are developed from FVT-anlage I (Figure 5D).

The marginal cirral anlagen are generated within the mid-portion and anterior of the parental right and left rows. Subsequently, marginal cirral anlagen developed into marginal cirri and completely replaced the parental ones (Figures 4M–P, 5B–D, F).

Three dorsal kinety anlagen (DKA) appear in the middle of the cell: one in the middle of the parental DK6 and the other two arise to the left sides (dorsal view) of parental DK1 and DK6. Subsequently, the leftmost DKA fragments at the middle region form four anlagen. With the proliferation of basal bodies, all six anlagen extend and form six DKs. Finally, a single caudal cirrus is differentiated at the posterior end of DK4, DK5, and DK6 each (Figures 4L–Q, 5A–G).

3.3.3 Molecular phylogeny

The SSU rRNA gene sequence of *T. aestuarina* n. sp. (GenBank accession no. OP173577) is 1,768 bp long and has a GC- content of 45.87%; that of *T. caudata* (GenBank accession no. OP173576) is 1,769 bp long and has a GC- content of 46.52%.

The topologies of ML and BI trees were nearly congruent; hence, only the ML tree was shown with nodal support from both methods (Figure 6). The fully supported clade formed by *T.*

caudata and two *T. pediculiformis* isolates (DQ057346 and MZ856309) is a sister clade to *T. aestuarina* n. sp., with low support (ML/BL, 45/0.73).

3.4 Species distributions

The species within *Trachelostyla* have a cosmopolitan distribution across more than 20 countries, on continents including Europe, Asia, North America, South America, and North Africa. They have been most frequently reported from Europe, but have not yet been recorded from Antarctica or Oceania (Figure 7). They are found mainly in marine or brackish water habitats such as islands, beaches, and intertidal zones. Only *T. caudata* has been reported once from freshwater, but no related morphological information was available (Agamaliev, 1986).

T. pediculiformis (Cohn, 1866) Borror, 1972, has been most frequently reported from Europe, Asia, North America, South America (Brazil), and Algeria in North Africa, while *T. caudata* has been recorded thus far only in Europe and Asia. *Trachelostyla rostrata* Lepsi, 1962, has thus far been reported only once from Romania in Europe and once from the Chesapeake Bay, East Coast of the United States in North America (Lepsi, 1962; Small and Lynn, 1985). The recently found *Trachelostyla multinucleata* Zhang et al., 2022, and the new species *T. aestuarina* n. sp. have thus far only been reported from China, with future work likely to expand the known biogeographic range to other continents.

4 Discussion

4.1 Establishment of *Trachelostyla aestuarina* n. sp. and comparison with congeners

According to Berger's revision, four species (*Trachelostyla canadiensis* Buitkamp and Wilbert, 1974; *Trachelostyla dubia* Dragesco, 1954; *Trachelostyla spiralis* Dragesco and Dragesco-Kernéis, 1986; and *Trachelostyla tani* Hu and Song, 2002) originally belonged to *Trachelostyla* and are now classified in other genera (Berger, 1999; Berger, 2008). Currently, there are only four valid species in the genus *Trachelostyla*: *T. pediculiformis*, *T. caudata*, *T. rostrata*, and *T. multinucleata*. Only *T. pediculiformis* and the recently reported *T. multinucleata* have detailed information on infraciliature.

T. aestuarina n. sp., *T. pediculiformis*, and *T. rostrata* all have a bipartite cell shape, e. g., a narrow neck-like constriction and a round posterior end and stable 11 frontal–ventral cirri (Gong et al., 2006; Berger, 2008; Zhang et al., 2022a). They could be distinguished by the number of macronuclear nodules (37–55 in *T. aestuarina* n. sp. *vs.* 9–17 in *T. pediculiformis* neotype and two in *T. rostrata*) and the cortical granules (present in *T. aestuarina* n. sp. *vs.* absent in *T. pediculiformis* neotype and *T. rostrata*).

Both *T. caudata* and *T. multinucleata* have many macronuclear nodules (greater than or equal to 20), similar to *T. aestuarina* n. sp. However, they can be easily distinguished from the new species by the following features.

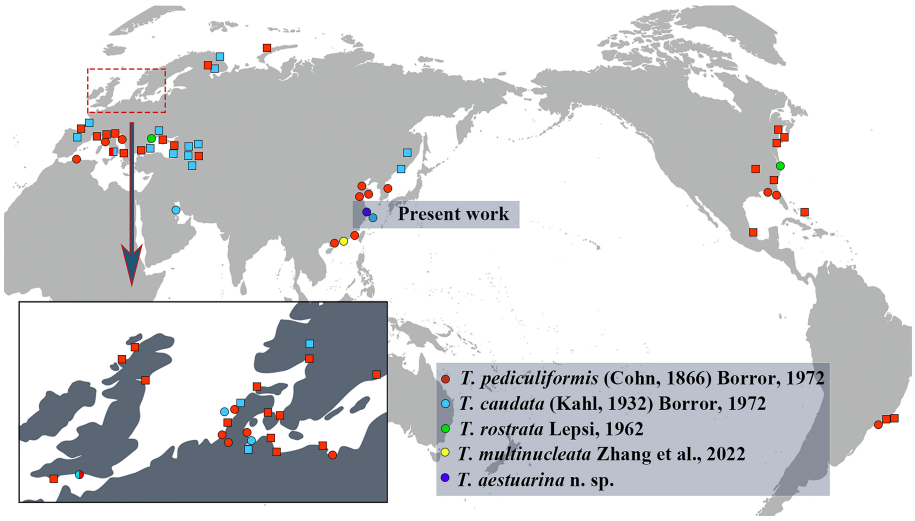

FIGURE 7
The current global geographic distribution records for the five valid *Trachelostyla* species. *Circles* indicate records with morphological data, while *squares* indicate records not substantiated by morphological data.

T. caudata, which is described in detail here, differs from *T. aestuarina* n. sp. in terms of cell shape (tripartite with a tail-like posterior end for *T. caudata vs*. bipartite with a round posterior end in *T. aestuarina* n. sp.), cell size *in vivo* (57–125 × 12–23 μm *vs*. 150–216 × 16–31 μm), the number of frontal–ventral cirri (10 *vs*. 11), and the cortical granules (absent *vs*. present).

T. multinucleata differs from *T. aestuarina* n. sp. in terms of its larger cell size (200–310 × 35–60 μm *vs*. 150–216 × 16–31 μm long *in vivo*), higher number of DKs (7 *vs*. 6), and no cortical granules (*vs*. present in *T. aestuarina* n. sp.) (Zhang et al., 2022a).

T. aestuarina n. sp. was not immediately observed from the Chinese type locality samples. It was only after the salinity increased that the ciliate was recorded. Ciliates are well documented as having a "preferred" ecological niche (Finlay and Esteban, 1998), along with the ability to exist cryptically in a ciliate "seed bank" until such environmental conditions (e.g., salinity) become favorable (Esteban and Finlay, 2003; Galotti et al., 2014). Ciliates can exist both in low numbers or simply be undetected in a given habitat or sample despite being present or even abundant, making the understanding of their actual biogeography challenging (Hines et al., 2022).

4.2 *Trachelostyla caudata* (Kahl, 1932) Borror, 1972

4.2.1 Comparison of the Chinese population with other *Trachelostyla caudata* populations

T. caudata was originally described from Germany by Kahl (1932), with a very brief description. *T. caudata* sensu Petran (1967) and sensu Al-Rasheid (2001) were classified as insufficient redescriptions (for details, see Berger, 2008), and only five marine populations remain with valid morphological data, despite numerous examples existing in the historic literature. However, none of the descriptions includes the clear ciliary pattern or molecular sequence data (Kahl, 1932; Kahl, 1933; Maeda and Carey, 1984; Carey, 1992; Al-Rasheid, 1999).

Although the number of cirri on the frontal region was mentioned (four or five, which is rather low compared with the type species), the value is questionable as some cirri (e.g., postoral ventral and pretransverse cirri) could have been overlooked since they are not easily detected *in vivo*. Therefore, we identified our form as *T. caudata* mainly based on the cell shape and the number of macronuclear nodules, although it has a slightly shorter cell length *in vivo* [57–125 μm, normally 100 μm, present study *vs*. 150–220 μm (Kahl, 1932), 120–240 μm (Kahl, 1933), 150 μm (Al-Rasheid, 1999, and Carey, 1992), and about 120 μm (Maeda and Carey, 1984)], which could be considered as an interpopulation variation.

According to Kahl (1932), there are 8–10 DKs, with cilia 12–15 μm long, while Maeda and Carey (1984) described the dorsal as shorter than that of *T. pediculiformis* (7–8 μm) (Gong et al., 2006; Zhang et al., 2022). The later description is consistent with our observations (six DKs, cilia 4–6 μm long *in vivo*).

4.2.2 Physiological reorganization

The process of morphogenetic and physiological reorganization has been investigated in *T. pediculiformis* and *T. multinucleata* (Gong et al., 2006; Shao et al., 2007; Zhang et al., 2022a). The generation pattern of the new ventral cirri is mainly consistent in the three species, except for the number of cirri generated by FVT-anlagen V (three in *T. caudata vs*. four in the others).

Concerning the formation of DKA, the leftmost DK anlage of *T. caudata* develops *de novo*, near the first parental kinety (*vs*. intrakinetally within kinety 1 in *T. pediculiformis* and *T. multinucleata*). For the other two anlagen, we suspect one develops intrakinetally in and one arises *de novo* left to parental kinety 6, considering they were clearly separated in an early stage. However, in *T. pediculiformis* and *T. multinucleata*, it was described as two parallel anlagen developing intrakinetally within kinety 6 (Shao et al., 2007; Zhang et al., 2022), which is uncommon in the morphogenesis of hypotrichs. Thus, more stages are needed to fully study the formation patterns of the new DKs. In all three species, each daughter cell has six new DKs, four from parental kinety 1 and two from kinety 6. However, *T. multinucleata* has seven DKs, while *Spirotrachelostyla tani* has only two. This variability in the number of DKs indicates that the DK formation pattern is not uniform within the trachelostylids.

4.3 Phylogenetic analyses

The phylogenetic tree constructed from the SSU rRNA gene sequences (Figure 6) showed that the family Trachelostylidae is monophyletic, which is consistent with previous studies (Huang et al., 2016; Zhang et al., 2022a). According to Berger (2008), the family Trachelostylidae contains only two genera, *Trachelostyla* and *Spirotrachelostyla* Gong et al., 2006, which share the following features: an elongate cell shape and a narrow neck-like constriction, adoral zone along the anterior and left margin of the head, straight and relatively short undulating membranes, and without dorsomarginal kineties. In the SSU rDNA phylogenetic trees, *Spirotrachelostyla* nested in the genus *Trachelostyla*, although with a low support (32/0.68). However, in previous multigene trees, it was robustly placed outside *Trachelostyla* (Zhang et al., 2022). Considering the unique spirally twisted cell and the higher number of cirri (about 13) scattered in the anterior peristolial region, *Spirotrachelostyla* is a morphologically well-supported genus. However, future work is needed to determine whether the genus, Trachelostyla is indeed monophyletic.

One *T. pediculiformis* population (KU594642) from Huang et al. (2016) was located at the base of the other major clade of the family Trachelostylidae, separated from the other two populations (DQ057346 and MZ856309). Considering it lacks morphological information, we agree that *T. pediculiformis* (KU594642) was likely a misidentification (Zhang et al., 2022a).

4.4 Key to the identification of the five species of *Trachelostyla*

1) Posterior cell portion narrowed tail-like..... 2
–Posterior cell portion broadly rounded.....3
2) Ten cirri in the frontal region.....*T. caudata*
–Eleven cirri in the frontal region.....*T. multinucleata*
3) Two macronuclear nodules.....*T. rostrata*
–More than two macronuclear nodules.....4
4) Cortical granules present.....*T. aestuarina*
–Cortical granules absent.....*T. pediculiformis*

4.5 Geographical distribution of *Trachelostyla*

The findings presented here support previous reports suggesting the cosmopolitan distribution of the genus *Trachelostyla*. *T. pediculiformis* and *T. caudata* have been reported most frequently and are the most widely distributed. There are several reasons for this, including: 1) more than half of these records are without morphological data; thus, misidentifications cannot be excluded; 2) *T. pediculiformis* and *T. caudata* were the first two species reported within the genus *Trachelostyla*, and it is possible that many species with only *in vivo* descriptions or illustrations could be incorrectly identified due to the highly similar morphological characteristics and the limited techniques used in early studies. It is equally possible that species present in a given region were simply not detected due to a large potential habitat area compared with limited researchers in the field. By providing detailed taxonomic data here combined with molecular sequences, future researchers in global regions will be able to compare their samples to the ciliates reported from China.

Data availability statement

The datasets presented in this study can be found in online repositories. The names of the repository/repositories and accession number(s) can be found below: https://www.ncbi.nlm.nih.gov/, OP173577 and OP173576; https://zoobank.org/References/e10ba883-fac7-4e81-8cb4-d521a945d99f.

Author contributions

ZZ performed the experiments and drafted the manuscript. HH and HP edited the manuscript. JJ conducted the writing—review and editing. All authors contributed to the article and approved the submitted version.

Funding

This work was supported by the Natural Science Foundation of China (project nos. 31772477 and 32170533) and NSFC Shiptime Sharing Project (project no. 42049903).

Acknowledgments

We would like to thank Mr. Haohao Lu (Shanghai Ocean University) for sampling and Prof. Weibo Song (Ocean University of China) for his helpful suggestions on the manuscript drafts.

Conflict of interest

The authors declare that the research was conducted in the absence of any commercial or financial relationships that could be construed as a potential conflict of interest.

Publisher's note

References

Agamaliev, F. G. (1986). Ciliates of the low-salinity lagoons of the Caspian Sea. *Arch. Protistenk.* 131 (3–4), 201–214. doi: 10.1016/S0003-9365(86)80042-2

Ahsan, R., Blanche, W., and Katz, L. A. (2022). Macronuclear development in ciliates, with a focus on nuclear architecture. *J. Eukaryot. Microbiol.* 69(5), e12898. doi: 10.1111/jeu.12898

Al-Rasheid, K. (1999). Free-living marine interstitial hypotrichid ciliates from jubail marine wildlife sanctuary in the Arabian gulf. *Agric. Sci.* 4 (1), 53–62. doi: 10.24200/jams.vol4iss1pp53-62

Al-Rasheid, K. A. S. (2001). New records of interstitial ciliates (Protozoa ciliophora) from the Saudi coasts of the red Sea. *Trop. Zool.* 14 (1), 133–156. doi: 10.1080/03946975.2001.10531148

Berger, H. (1999). Monograph of the oxytrichidae (Ciliophora, hypotrichia). *Monogr. Biol.* 78, 1–1080. doi: 10.1007/978-94-011-4637-1

Berger, H. (2008). Monograph of the amphisiellidae and trachelostylidae (Ciliophora, hypotricha). *Monogr. Biol.* 88, 1–737. doi: 10.1007/978-1-4020-8917-6

Borror, A. C. (1972). Revision of the order hypotrichida (Ciliophora, Protozoa). *J. Protozool.* 19 (1), 1–23. doi: 10.1111/j.1550-7408.1972.tb03407.x

Carey, P. G. (1992). *Marine interstitial ciliates. an illustrated key* (New York, NY: Chapman & Hall).

Castresana, J. (2000). Selection of conserved blocks from multiple alignments for their use in phylogenetic analysis. *Mol. Biol. Evol.* 17 (4), 540–552. doi: 10.1093/oxfordjournals.molbev.a026334

Chen, L., Dong, J., Wu, W., Xin, Y., Warren, A., Ning, Y., et al. (2020). Morphology and molecular phylogeny of a new hypotrich ciliate, *Anteholosticha songi* nov. spec., and an American population of *Holosticha pullaster* (Muller 1773) foissner et al. 1991 (Ciliophora, hypotrichia). *Eur. J. Protistol.* 72, 125646. doi: 10.1016/j.ejop.2019.125646

Chen, L., Ren, Y., Han, K., Stoeck, T., Jiang, J., and Pan, H. (2022). Redescription of two free-swimming peritrichs, *Hastatella aesculacantha* and *H. radians* (Ciliophora, peritrichia), with note on the phylogeny of the genus *Hastatella*. *Eur. J. Protistol.* 84, 125891. doi: 10.1016/j.ejop.2022.125891

Esteban, G. F., and Finlay, B. J. (2003). Cryptic freshwater ciliates in a hypersaline lagoon. *Protist* 154 (3-4), 411–418. doi: 10.1078/143446103322454149

Finlay, B. J., and Esteban, G. F. (1998). Planktonic ciliate species diversity as an integral component of ecosystem function in a freshwater pond. *Protist* 149 (2), 155–165. doi: 10.1016/S1434-4610(98)70020-3

Galotti, A., Finlay, B. J., Jiménez-Gómez, F., Guerrero, F., and Esteban, G. F. (2014). Most ciliated protozoa in extreme environments are cryptic in the 'seed bank'. *Aquat. Microbial. Ecol.* 72 (3), 187–193. doi: 10.3354/ame01699

Gong, J., Song, W., Li, L., Shao, C., and Chen, Z. (2006). A new investigation of the marine ciliate, *Trachelostyla pediculiformis* (Cohn 1866) borror 1972 (Ciliophora, hypotrichida), with establishment of a new genus, *Spirotrachelostyla* nov. gen. *Eur. J. Protistol.* 42 (1), 63–73. doi: 10.1016/j.ejop.2005.12.001

Hines, H. N., McCarthy, P. J., and Esteban, G. F. (2022). A case building ciliate in the genus *pseudoblepharisma* found in subtropical fresh water. *Diversity* 14 (3), 174. doi: 10.3390/d14030174

Huang, J., Luo, X., Bourland, W. A., Gao, F., and Gao, S. (2016). Multigene-based phylogeny of the ciliate families amphisiellidae and trachelostylidae (Protozoa: Ciliophora: Hypotrichia). *Mol. Phylogenet. Evol.* 101, 101–110. doi: 10.1016/j.ympev.2016.05.007

Kahl, A. (1932). Urtiere oder Protozoa i. wimpertiere oder ciliata (Infusoria) III. spirotricha. *Tierwelt. Dtl.* 25, 399–650.

Kahl, A. (1933). "Ciliata libera et ectocommensalia," in *Die tierwelt der nord- und ostsee*. Eds. G. Grimpe and E. Wagler (Leipzig: Teil II. c3) 23, 184–226.

Kim, K. S., Ji, S. J., and Min, G. S. (2020). COI DNA barcoding for *Sterkiella multicirrata* (Ciliophora: Oxytrichidae) from south Korea. *Anim. Syst. Evol. Divers.* 36 (1), 7–9. doi: 10.5635/ASED.2020.36.1.025

Lepsi, I. (1962). Über einige insbesondere psammobionte ciliaten vom rumänischen schwarzmeer-ufer. *Zool. Anz.* 168, 460–465.

Li, J., Wang, Y., Zhang, H., Al-Farraj, S. A., Shao, C., and Wang, J. (2021). Morphology, ontogeny and molecular phylogeny of a new urostylid ciliate, *Bakuella* (*Pseudobakuella*) *guangdongica* n. sp. (Ciliophora, hypotrichia) from southern China. *Eur. J. Protistol.* 81, 125795. doi: 10.1016/j.ejop.2021.125795

Luo, X., Bourland, W. A., Song, W., and Huang, J. (2021). New contributions to the taxonomy of urostylid ciliates (Ciliophora, hypotrichia), with establishment of a new genus and new species. *Eur. J. Protistol.* 80, 125810. doi: 10.1016/j.ejop.2021.125810

Lynn, D. H. (2008). *The ciliated Protozoa: Characterization, classification, and guide to the literature* (Dordrecht: Springer).

Maeda, M., and Carey, P. G. (1984). A revision of the genera *Trachelostyla* and *Gonostomum* (Ciliophora, hypotrichida), including redescriptions of *T. pediculiformis* (Cohn 1866) kahl 1932 and *T. caudata* Kahl 1932. *Bull. Br. Mus. Nat. Hist. (Zool.).* 47, 1–17.

Medlin, L., Elwood, H. J., Stickel, S., and Sogin, M. L. (1988). The characterization of enzymatically amplified eukaryotic 16S-like rRNA-coding regions. *Gene* 71 (2), 491–499. doi: 10.1016/0378-1119(88)90066-2

Miller, M. A., Pfeiffer, W., and Schwartz, T. (2011). "The CIPRES science gateway: a community resource for phylogenetic analyses," in *Proceedings of the 2011 TeraGrid conference: extreme digital discovery* (Salt Lake City, Utah, ACM New York, NY, USA.), 1–8.

Obert, T., and Vďačný, P. (2020). Evolutionary origin and host range of *Plagiotoma lumbrici* (Ciliophora, hypotrichia), an obligate gut symbiont of lumbricid earthworms. *Eur. J. Protistol.* 67 (2), 176–189. doi: 10.1111/jeu.12768

Omar, A., Yeo, J. H., and Jung, J.-H. (2022). A new "flagship" ciliate, *Pseudostylonychia obliquocaudata* n. gen., n. sp.(Ciliophora, hypotricha), from south Korea. *Eur. J. Protistol.* 84, 125893. doi: 10.1016/j.ejop.2022.125893

Paiva, T. (2020). Systematic redefinition of the hypotricha (Alveolata, ciliophora) based on combined analyses of morphological and molecular characters. *Protist* 171 (4), 125755. doi: 10.1016/j.protis.2020.125755

Pan, X., Bourland, W. A., and Song, W. (2013). Protargol synthesis: an in-house protocol. *J. Eukaryot. Microbiol.* 60 (6), 609–614. doi: 10.1111/jeu.12067

Park, K. M., Jung, J. H., Kim, J. H., Min, G. S., and Kim, S. (2020). Morphology, morphogenesis, and molecular phylogeny of a new freshwater ciliate, *Gonostomum jangbogoensis* n. sp. (Ciliophora, hypotricha), from Victoria land, Antarctica. *Eur. J. Protistol.* 73, 125669. doi: 10.1016/j.ejop.2019.125669

Petran, A. (1967). Certecari asupra faunei de ciliate psamobionte la plajele dn sudul litoralulu romanesc al marii negre. *Ecol. Mar.* 2, 169–191.

Rambaut, A. (2018). *"FigTree, a graphical viewer of phylogenetic trees (Version 1.4. 4)"*. Institute of Evolutionary Biology, University of Edinburgh. Available at: https://github.com/rambaut/figtree/releases/tag/v1.4.4

Ronquist, F., Teslenko, M., van der Mark, P., Ayres, D. L., Darling, A., Höhna, S., et al. (2012). MrBayes 3.2: efficient Bayesian phylogenetic inference and model choice across a large model space. *Syst. Biol.* 61 (3), 539–542. doi: 10.1093/sysbio/sys029

Shao, C., Song, W., Yi, Z., Gong, J., Li, J., and Lin, X. (2007). Morphogenesis of the marine spirotrichous ciliate, *Trachelostyla pediculiformis* (Cohn 1866) (Ciliophora, stichotrichia), with consideration of its phylogenetic position. *Eur. J. Protistol.* 43 (4), 255–264. doi: 10.1016/j.ejop.2007.01.004

Small, E. B., and Lynn, D. H. (1985). "Phylum ciliophora doflein 1901," Lee, J. J., Hutner, S. H., and Bovee, E. C. (eds.). *An illustrated guide to the protozoa*. (Lawrence, Kansas: Society of Protozoologists).

Song, W., Zhang, T., Zhang, X., Warren, A., Song, W., Zhao, Y., et al. (2021). Taxonomy, ontogenesis and evolutionary relationships of the algae-bearing ciliate *Bourlandella viridis* (Kahl 1932) comb. nov., with establishment of a new genus and new family (Protista, ciliophora, hypotrichia). *Front. Microbiol.* 11. doi: 10.3389/fmicb.2020.560915

Stamatakis, A. (2014). RAxML version 8: a tool for phylogenetic analysis and post-analysis of large phylogenies. *Bioinformatics* 30 (9), 1312–1313. doi: 10.1093/bioinformatics/btu033

Tamura, K., Stecher, G., and Kumar, S. (2021). MEGA11: molecular evolutionary genetics analysis version 11. *Mol. Biol. Evol.* 38 (7), 3022–3027. doi: 10.1093/molbev/msab120

Timmons, C. M., Shazib, S. U., and Katz, L. A. (2022). Epigenetic influences of mobile genetic elements on ciliate genome architecture and evolution. *J. Eukaryot. Microbiol.* 69(5), e12891. doi: 10.1111/jeu.12891

Vďačný, P., and Foissner, W. (2021). Morphology and ontogenesis of two new *Hemiholosticha* species (Ciliophora, hypotrichia, hemiholostichidae nov. fam.). *Eur. J. Protistol.* 77, 125763. doi: 10.1016/j.ejop.2020.125763

Valentine, M. S., and Van Houten, J. (2022). Ion channels of cilia: *Paramecium* as a model. *J. Eukaryot. Microbiol.* 69(5), e12884. doi: 10.1111/jeu.12884

Wilbert, N. (1975). Eine verbesserte technik der protargolimprägnation für ciliaten. *Mikrokosmos* 64, 171–179.

Wu, W., Dong, J., Long, Y., Warren, A., Chen, L., and Qiu, H. (2022). Redescription and phylogenetic position of the terrestrial ciliates *Gastrostylides dorsicirratus* and *Heterourosomoida lanceolata* (Hypotricha, dorsomarginalia). *Eur. J. Protistol.* 82, 125859. doi: 10.1016/j.ejop.2021.125859

Xu, W., Ma, J., Li, Y., Bourland, W. A., Petroni, G., Luo, X., et al. (2022). Phylogeny of a new ciliate family clampidae fam. nov. (Protista: Ciliophora), with notes on morphology and morphogenesis. *Zool. J. Linn. Soc.* 196(1), 88–104. doi: 10.1093/zoolinnean/zlab102

Zhang, X., Lu, X., Chi, Y., Jiang, Y., Wang, C., Al-Farraj, S. A., et al. (2022b). Timing and characteristics of nuclear events during conjugation and genomic exclusion in *Paramecium multimicronucleatum*. *Mar. Life Sci. Technol.* 4 (3), 317–328. doi: 10.1007/s42995-022-00137-y

Zhang, T., Shao, C., Song, W., Vd'ačný, P., Al-Farraj, S., and Wang, Y. (2022a). Multi-gene phylogeny of the ciliate genus *Trachelostyla* (Ciliophora, hypotrichia), with integrative description of two species, *Trachelostyla multinucleata* spec. nov. and *T. pediculiformis* (Cohn 1866). *Front. Microbiol.* 12. doi: 10.3389/fmicb.2021.775570